Transpositional scaling and niche transitions restore organ size and shape during zebrafish fin regeneration

Scott Stewart[1,*,#], Gabriel A. Yette[1,2,#], Astra L. Henner[1], Heather K. Le Bleu[1,2], Joshua A. Braunstein[1,2], Jad W. Chehab[1], Michael J. Harms[1,3] and Kryn Stankunas[1,2,*]

Short title: Fin skeletal geometry provides positional information instructing regenerative growth

[1]Institute of Molecular Biology
[2]Department of Biology
[3]Department of Chemistry and Biochemistry
University of Oregon
273 Onyx Bridge
1318 Franklin Blvd
Eugene, OR 97403-1229
Office: (541) 346-7416
Fax: (541) 346-4854

* Correspondence: kryn@uoregon.edu; sstewar2@uoregon.edu

# Equal contributions

ABSTRACT

Adult fish fins regenerate to their original size and shape regardless of the nature or position of the injury. Spallanzani, Broussonet and Morgan initiated the pursuit of this scaling mystery of appendage regeneration in the 17th and 18th centuries. They and later researchers found the rate of regeneration initially correlates with the amount of tissue removed and then progressively decreases until outgrowth stops as the appendage's form is restored. Prevailing models speculate that appendage cells harbor positional identities that instruct differential outgrowth after injury. We revisited Morgan's fin resection experiments using the zebrafish model and show that differential Wnt production by distal niche cell populations determines the extent of regeneration. We identify Dachshund transcription factors as niche markers and show that the niche forms from intra-ray mesenchyme that populates the inside of the cylindrical and progressively tapered fin rays. The niche, and consequently Wnt, steadily dissipates as regeneration proceeds; once exhausted, growth stops. Supported by mathematical modeling, we show *longfin*^{t2} zebrafish regenerate exceptionally long fins due to a broken niche "countdown timer". We conclude that regenerated fin size is dictated by the amount of niche formed upon damage – which is simply dependent on the availability of intra-ray mesenchyme defined by bone girth at the injury site. This "transpositional scaling" model contends mesenchyme-niche state transitions and self-restoring skeletal geometry, not individual cell memories, determine a regenerated fin's size and shape.

One Sentence Summary

Skeletal geometry provides the positional information for restoring organ size during appendage regeneration.

65

MAIN TEXT

Regenerating organs restore their original size and shape after injury. Vertebrate appendage regeneration, including that of teleost fish fins, provides a striking example of this phenomenon. Major fin amputations, tiny resections, and cuts of diverse geometry all produce the same outcome – a restored fin matching the original's form and in scale with the animal's body. Spallanzani, Broussonet, and T. H. Morgan pioneered studies of this longstanding mystery of regeneration in the 18th and 19th centuries (Broussonet, 1786; Morgan, 1900). For example, Morgan used oblique caudal fin resections to show that regeneration rates initially correlate with the amount of tissue lost and then progressively slow, ultimately stopping growth when the original size is regained (Morgan, 1900). Tissue adjacent to damage sites seemingly interprets Cartesian coordinate-like positional information to trigger the appropriate rate and extent of re-growth. Further, the process of regeneration must restore the same diverse positional qualities.

Prevailing models, now largely derived from zebrafish studies, hold that fin cells harbor molecularly-encoded identities leading to differential cell proliferation depending on amputation position (Nachtrab et al., 2013; Rabinowitz et al., 2017; Rolland-Lagan et al., 2012; Tornini et al., 2016). This concept requires an extensive array of cellular identities, some epigenetic mechanism for cells to store those identities, and, perhaps most vexing, for the positional information to be restored during the regeneration process. Ultimately, however, the rate and extent of outgrowth is dictated by production of growth factors, including FGF (Lee et al., 2005; Poss et al., 2000a; Shibata et al., 2016; Whitehead et al., 2005) and Wnt (Kawakami et al., 2006; Stewart et al., 2014; Stoick-Cooper et al., 2007; Wehner et al., 2014), with the net effect of promoting cellular proliferation. Therefore, understanding growth factor production dynamics provides a logical entry to uncover fin size and shape restoration mechanisms.

Wnt signals indirectly promote cell proliferation (Wehner et al., 2014), including by maintaining progenitor cells of the bone-producing osteoblast lineage (Stewart et al., 2014), to drive outgrowth until the fin is fully restored. Several Wnts including *wnt5a*, *wnt5b*, and *wnt10a* are produced in the distal regenerating fin, including by distal blastema cells that we term the distal niche (Kawakami et al., 2006; Poss et al., 2000b; Stewart et al., 2014; Stoick-Cooper et al., 2007; Wehner et al., 2014). We hypothesized differential Wnt production determines the rate and ultimately extent of regeneration. Revisiting Morgan's experiments, we obliquely amputated adult zebrafish fins from the distal tip of the dorsal side to a proximal location ventrally (see Fig. S1 for fin amputation planes and anatomical definitions) (Morgan, 1900). We then variably inhibited Wnt secretion by graded dosing of low concentrations of Wnt-C59 (Proffitt et al., 2013; Stewart et al., 2014). Partial perturbation of Wnt signaling prevented dorsal but not ventral tissue regeneration (Fig. 1A-E). Similarly, medial tissue was more sensitive than lateral tissue to Wnt inhibition following perpendicular resections (Fig. S2). We conclude differential Wnt production underlies reacquisition of the stereotypical shape of a zebrafish fin. Concordantly, levels of *wnt5a*, a representative niche-expressed Wnt, correlated with the demand for regenerative growth along the proximal-distal axis four days after oblique fin amputations (Fig. 1F, G).

Wnt signaling "strength" could be encoded either by the amount of Wnt produced per niche cell or the number of Wnt-producing niche cells. Regardless, we reasoned that understanding the properties of niche cells was key to deciphering size control mechanisms. We used RNA-Seq of 4 days post amputation (dpa) distal vs. proximal fin regenerates, as demarcated by the distal epidermal marker Tg(*shha:EGFP)* (Ertzer et al., 2007), to identify niche-characterizing factors (Fig. S3). The *dachshund* (*dach*) family transcription factors (Mardon et al., 1994; Shen and Mardon, 1997) *dacha* (5.9-fold) and *dachc* (6.0-fold) were notably distally

enriched (Fig. S3). *dachc* mimicked *wnt5a* in having notably higher expression levels in 4 dpa proximal tissue of diagonally amputated regenerating fins (Fig. 1H, I).

We used antibody staining to conclusively identify caudal fin cells that express Dacha/c (hereafter referred to as Dach) over the course of fin regeneration (Fig. 1J-O). Dach-expressing cells were rarely observed before 3 days post amputation (dpa) (Fig. 1J). At 3 dpa, Dach became robustly expressed in distal cells adjacent to, but distinct from, distal Runx2^{+} pre-osteoblasts (Fig. 1K). These Dach^{+} niche cells then steadily reduced over the course of regeneration to a small residual population also found in distal tissue of unamputated fins (Fig. 1L-O). We conclude that Dach transcription factors specifically mark Wnt-producing niche cells throughout the course of regeneration. The three-day delay prior to the appearance of Dach^{+} niche corresponds with the view that fin regeneration proceeds by an acute injury repair phase followed by a prolonged period of progressive outgrowth (Chen and Poss, 2017). Finally, differential numbers of niche cells produced upon injury and then maintained through regeneration likely accounts for our observation that variable Wnt strength underlies fin outgrowth extents.

Canonical Wnt/β-catenin signaling during fin regeneration is confined to distal blastema / niche cells and pre-osteoblasts in which it indirectly promotes further proximal mesenchyme proliferation (Wehner et al., 2014) and maintains a progenitor state (Stewart et al., 2014), respectively. However, a potential role for Wnt in maintaining the niche pool itself is unexplored. Using the new Dach marker, we found that pan-Wnt inhibition initiated at 4 dpa using Wnt-C59 rapidly depleted niche cells (Fig. S4). Wnt inhibition prevented outgrowth but did not disrupt osteoblast differentiation, joint formation, or skeletal maturation, reinforcing our previous insight that Wnt/β-catenin promotes bone progenitor maintenance upstream of and in

135 opposition to differentiation (Stewart et al., 2014). Wnt, whether canonical or non-canonical, appears to have an analogous autocrine role – maintaining the niche population in a state whereby it can orchestrate continued regeneration.

The loss of niche cells upon Wnt inhibition allowed us to test if artificial depletion of the niche pool mimics normal termination of regeneration – as supported by our observation that 140 Dach$^+$ niche cells progressively decrease over regeneration. Wnt inhibition irreversibly blocked fin regeneration, with only rare outgrowth seen long after drug removal (Fig. S4). In contrast, re-amputating Wnt-inhibited fins immediately re-initiated regeneration. Small molecule inhibition of FGF receptor signaling prevented outgrowth to the same degree as Wnt inhibition (Fig. S4). However, as FGF inhibition did not deplete Dach$^+$ niche cells (Fig. S4), regeneration resumed 145 following drug washout, matching previous observations (Lee et al., 2005). Therefore, mitogenic FGF, which appears niche-expressed (Whitehead et al., 2005) and is Wnt-dependent (Wehner et al., 2014), acts downstream of Wnt's niche maintenance role. Niche cell numbers then set dynamic levels of both signaling proteins and therefore outgrowth rate. Regeneration ceases when the niche pool, and correspondingly Wnt and FGF production, depletes below an effective 150 level. These observations underscore that understanding instructive growth control mechanisms requires revealing niche cell origins and fates.

Regenerated fin tissues are derived from progenitor cells formed by de-differentiation of mature cells extant at the injury site (Chen and Poss, 2017). We used a mosaic lineage tracing system to permanently label different cell populations in uninjured fins (Stewart and Stankunas, 155 2012) and then track which lineage generates Dach$^+$ niche cells during regeneration. Intra-ray mesenchyme, cells within the cylindrically-shaped bony rays, generated nearly all Dach$^+$ niche cells (Fig. 2A-D). A major population of regenerative blastema cells are derived from intra-ray

mesenchymal cells that upregulate *tryptophan hydroxylase 1b* (*tph1b*) upon injury (Tornini et al., 2016). We found most Dach^{+} niche cells shared this lineage using the *Tg(tph1b-mCherry)*
160 reporter line (Tornini et al., 2016) (Fig. 2E-F). Likewise, only the distal-most Msx-expressing blastema cells were Dach-positive (Fig. 2G). The mesenchymal cell state marker Snail (Lamouille et al., 2014) was expressed in non-injured intra-ray mesenchyme and proximal blastema cells (Fig. 2H, I). In contrast, Snail was absent from Dach^{+} niche cells except for a small population of transitioning double Dach^{+}/Snail^{+} cells at the boundary (Fig. 2I).
165 Concordantly, *snai2* transcripts were abundant in blastema mesenchyme except the distal-most tissue (Fig. S5). These observations support a cyclical model whereby fin amputation induces a delayed transition of Snail^{+} intra-ray mesenchyme to a Dach^{+} niche state (Fig. 2J, K; S6). The Dach-expressing niche cells then progressively convert back to Snail^{+} mesenchyme that re-populates regenerated ray bones.

170 The origin of niche cells from intra-ray mesenchyme led us to consider that skeletal geometry might instruct how much niche is formed upon amputation. By this model, resecting a larger bone, with a relatively high volume capacity for mesenchyme, would produce a larger initial niche population and therefore more regeneration. In support, the size of fin ray bone segments noticeably tapers along the proximal-to-distal axis (Fig. 3A-E). Further, longer lateral
175 rays are wider at their base than shorter medial rays. We measured the radius of the medial sixteen rays at a fixed proximal-distal position and then plotted the squared values (as a proportional surrogate for bone segment cylindrical volume) as adjacent bars. The V-shape formed by the bars' distribution neatly matched that of a zebrafish fin by closely approximating distributed ray lengths (Fig. 3A).

180 This model predicts niche amount should vary by proximal-distal amputation position, correlating with the tapering bony rays. Whole-mount in situ hybridization for *dachc* transcripts at 3 dpa revealed that proximal amputations produced large *dachc*-expressing niche pools while distal cuts generated progressively smaller niches (Fig. 3F-H). Further, *dachc* expression across the dorsal-to-ventral fin axis correlated with regenerative demand upon perpendicular resections
185 (Fig. S7) – as with diagonal amputations (Fig. 1H, I). Lateral regions that re-form the longest rays expressed high levels of *dachc*. In contrast, medial tissue that generates short rays to restore the original V-shaped fin produced small *dachc*-marked niches. Progressive niche depletion – shown by Dach$^+$ expression over a regeneration time course (Fig. 1J-O) – slows then terminates outgrowth. Further, as a depleting niche would sustain a diminishing pre-osteoblast pool,
190 regenerating bone size would progressively contract and therefore restore a tapered skeletal ray.

We used mathematical modeling to further explore if skeletal geometry coupled with progressive niche depletion could account for robust size restoration during fin regeneration. We started by assuming, at any given time, outgrowth rate is proportional to the number of distal niche cells. We considered that niche cells both proliferate and convert back to mesenchyme.
195 This logic establishes a "countdown timer" if the niche collectively re-differentiates faster than it proliferates. The number of initial niche cells sets the timer, which then ends when the niche population depletes below some fixed, effective level. We modeled that the bone area exposed upon ray resection, as a linear proxy for cylinder volume, determines the number of initial niche cells. As such, ray bone size at the amputation site ultimately instructs regenerated ray length.

200 We solved differential equations to derive a final equation describing regenerated ray length as a function of the ray radius at the amputation position:

$$l(t_{end}) = \frac{k_l}{\alpha}(N_\Phi - \beta\pi r^2)$$

where k_l is the rate of length growth per niche cell, α is the difference in niche cell growth rate versus rate of differentiation back to intra-ray mesenchymal cells, N_Φ is the number of niche cells below which growth stops, and β is the number of niche cells released per bone cross-sectional area. Mathematically exploring the formula reinforced the conclusion that α must be negative to provide net niche depletion. Solving expected regenerated ray lengths using measured ray radii and optimized constants produced a distribution largely matching actual measured lengths (Fig. 3I) – naturally matching normalized radius^2 distributions. The linear relationship between bone radius squared and remaining ray length from the measurement position held across the proximal-distal fin axis (Fig. 3J, R-squared = 0.7). Likewise, existent bone lengths from a hypothetical injury point largely matched theoretical regenerated lengths derived from radius measurements and our growth equation (Fig. 3K).

Several zebrafish mutants develop and regenerate long fins, including dominant *longfin*^{t2} (Van Eeden et al., 1996), well known as one of two mutations characterizing the *Tüpfel longfin* (*TL*) strain (Haffter et al., 1996) (Fig. 4A, B). *longfin*^{t2} ray radius measurements predicted overall fin shape but greatly under-anticipated ray lengths (Fig. 4C). Therefore, the skeleton was not proportionally re-scaled during development and instead suggesting *longfin*^{t2} disrupts a fin outgrowth regulatory mechanism. We used our mathematical model to predict the growth-determining parameter disrupted in *longfin*^{t2} fish. The cell proliferation rate (k_l) could be larger (e.g. increased mitogen production or mitogen sensitivity), β could be larger, establishing a larger niche pool upon injury, or α could be "less negative", leading to niche perdurance. Changing k_l or β vs. α had distinct theoretical effects when plotting expected regenerative growth over time and growth rate over time (Fig. 4D, E). Following amputation, *longfin*^{t2} fish showed prolonged regenerative growth rather than increased initial growth or peak growth rate

225 (Fig. 4F, G; S8), suggesting they have a persistent niche (less negative α) rather than enhanced niche generation (β) or increased cellular growth rate (k_l).

We examined *dachc* expression in *longfin*^{t2} heterozygotes following fin resection to see if niche dynamics were disrupted as anticipated by our modeling (Fig. 4H-Q). *longfin*^{t2} fish initially formed a normal-sized niche. However, unlike wildtype clutchmates, their *dachc*-expressing
230 niche only slowly depleted, implicating a less negative α constant. Finally, increasing α while inputting *longfin*^{t2} ray radii measurements in our formula now largely predicted actual *longfin*^{t2} regenerated ray lengths (Fig. S9). These results support the robustness of our model and show that *longfin*^{t2} disrupts the niche depletion system.

We conclude transposition of ray widths into lengths by niche generation, with
235 subsequent steady niche depletion, returns the regenerated fin to its original size. As niche activity, defined by Wnt production, also impacts pre-osteoblast output, positional information stored in skeletal geometry is self-restoring. In other words, a depleting niche directs both progressively slower outgrowth and narrower bones as Wnt production lessens and hence maintains a smaller pre-osteoblast pool. We use the term "transpositional scaling" to describe
240 this model for organ size determination – a new answer to an age-old question of appendage regeneration.

Vertebrate appendage regeneration, including that in zebrafish fins, is espoused as compelling evidence for pattern formation by Cartesian coordinate-defined cellular positional identities (Wolpert, 2016). However, our transpositional scaling model does not require fin cells
245 to retain any such molecular information or downstream morphogen gradients. Similarly, the hypothesized "pre-pattern" established early in a regenerating blastema that directs regional outgrowth (Nachtrab et al., 2013; Rabinowitz et al., 2017; Rolland-Lagan et al., 2012; Tornini et

al., 2016) can be explained by skeletal geometry-defined niche cell numbers alone. The state transition mechanisms that generate the niche and drive its progressive depletion are then identical throughout the fin but produce differential, predictable output depending on the starting condition.

Could similar models apply in other circumstances where an organ is restored to scale? Progenitor cell supporting-niche populations are a common component of organ growth, homeostasis, and regeneration (Chacón-Martínez et al., 2018; Yamashita and Tumbar, 2014). Our simple model, inherently dependent on regulatory networks with the positional information stored in tissue geometry rather than molecular information, establishes a compelling paradigm to explore in many contexts.

REFERENCES

Broussonet, M. (1786). Observations sur la régénération de quelques parties du corps des poissons. Histoire De lAcadémie Royale Des Sciences 684–688.

Chacón-Martínez, C.A., Koester, J., and Wickström, S.A. (2018). Signaling in the stem cell niche: regulating cell fate, function and plasticity. Development *145*, dev165399.

Chen, C.-H., and Poss, K.D. (2017). Regeneration Genetics. Annu. Rev. Genet. *51*, 63–82.

Ertzer, R., Müller, F., Hadzhiev, Y., Rathnam, S., Fischer, N., Rastegar, S., and Strähle, U. (2007). Cooperation of sonic hedgehog enhancers in midline expression. Developmental Biology *301*, 578–589.

Haffter, P., Odenthal, J., Mullins, M.C., Lin, S., Farrell, M.J., Vogelsang, E., Haas, F., Brand, M., Van Eeden, F.J., Furutani-Seiki, M., et al. (1996). Mutations affecting pigmentation and shape of the adult zebrafish. Dev. Genes Evol. *206*, 260–276.

Kawakami, Y., Rodriguez Esteban, C., Raya, M., Kawakami, H., Martí, M., Dubova, I., and Izpisúa Belmonte, J.C. (2006). Wnt/beta-catenin signaling regulates vertebrate limb regeneration. Genes Dev. *20*, 3232–3237.

Lamouille, S., Xu, J., and Derynck, R. (2014). Molecular mechanisms of epithelial-mesenchymal transition. Nat Rev Mol Cell Biol *15*, 178–196.

Lee, Y., Grill, S., Sanchez, A., Murphy-Ryan, M., and Poss, K.D. (2005). Fgf signaling instructs position-dependent growth rate during zebrafish fin regeneration. Development *132*, 5173–5183.

Mardon, G., Solomon, N.M., and Rubin, G.M. (1994). dachshund encodes a nuclear protein required for normal eye and leg development in Drosophila. Development *120*, 3473–3486.

Morgan, T.H. (1900). Regeneration in teleosts. Archiv Für Entwicklungsmechanik Der Organismen *10*, 120–134.

Nachtrab, G., Kikuchi, K., Tornini, V.A., and Poss, K.D. (2013). Transcriptional components of anteroposterior positional information during zebrafish fin regeneration. Development *140*, 3754–3764.

Poss, K.D., Shen, J., Nechiporuk, A., McMahon, G., Thisse, B., Thisse, C., and Keating, M.T. (2000a). Roles for Fgf signaling during zebrafish fin regeneration. Developmental Biology *222*, 347–358.

Poss, K.D., Shen, J., and Keating, M.T. (2000b). Induction of lef1 during zebrafish fin regeneration. Dev. Dyn. *219*, 282–286.

Proffitt, K.D., Madan, B., Ke, Z., Pendharkar, V., Ding, L., Lee, M.A., Hannoush, R.N., and Virshup, D.M. (2013). Pharmacological inhibition of the Wnt acyltransferase PORCN prevents growth of WNT-driven mammary cancer. Cancer Res. *73*, 502–507.

Rabinowitz, J.S., Robitaille, A.M., Wang, Y., Ray, C.A., Thummel, R., Gu, H., Djukovic, D., Raftery, D., Berndt, J.D., and Moon, R.T. (2017). Transcriptomic, proteomic, and metabolomic landscape of positional memory in the caudal fin of zebrafish. Proc. Natl. Acad. Sci. U.S.a. *114*, E717–E726.

Rolland-Lagan, A.-G., Paquette, M., Tweedle, V., and Akimenko, M.-A. (2012). Morphogen-based simulation model of ray growth and joint patterning during fin development and regeneration. Development *139*, 1188–1197.

Shen, W., and Mardon, G. (1997). Ectopic eye development in Drosophila induced by directed dachshund expression. Development *124*, 45–52.

Shibata, E., Yokota, Y., Horita, N., Kudo, A., Abe, G., Kawakami, K., and Kawakami, A. (2016). Fgf signalling controls diverse aspects of fin regeneration. Development *143*, 2920–2929.

Stewart, S., and Stankunas, K. (2012). Limited dedifferentiation provides replacement tissue during zebrafish fin regeneration. Developmental Biology *365*, 339–349.

Stewart, S., Gomez, A.W., Armstrong, B.E., Henner, A., and Stankunas, K. (2014). Sequential and opposing activities of Wnt and BMP coordinate zebrafish bone regeneration. Cell Reports *6*, 482–498.

Stoick-Cooper, C.L., Weidinger, G., Riehle, K.J., Hubbert, C., Major, M.B., Fausto, N., and Moon, R.T. (2007). Distinct Wnt signaling pathways have opposing roles in appendage regeneration. Development *134*, 479–489.

Tornini, V.A., Puliafito, A., Slota, L.A., Thompson, J.D., Nachtrab, G., Kaushik, A.-L., Kapsimali, M., Primo, L., Di Talia, S., and Poss, K.D. (2016). Live Monitoring of Blastemal Cell Contributions during Appendage Regeneration. Curr. Biol. *26*, 2981–2991.

Van Eeden, F.J., Granato, M., Schach, U., Brand, M., Furutani-Seiki, M., Haffter, P., Hammerschmidt, M., Heisenberg, C.P., Jiang, Y.J., Kane, D.A., et al. (1996). Genetic analysis of fin formation in the zebrafish, Danio rerio. Development *123*, 255–262.

Wehner, D., Cizelsky, W., Vasudevaro, M.D., Özhan, G., Haase, C., Kagermeier-Schenk, B., Röder, A., Dorsky, R.I., Moro, E., Argenton, F., et al. (2014). Wnt/β-catenin signaling defines organizing centers that orchestrate growth and differentiation of the regenerating zebrafish caudal fin. Cell Reports *6*, 467–481.

Whitehead, G.G., Makino, S., Lien, C.-L., and Keating, M.T. (2005). fgf20 is essential for initiating zebrafish fin regeneration. Science *310*, 1957–1960.

Wolpert, L. (2016). Positional Information and Pattern Formation. Curr. Top. Dev. Biol. *117*, 597–608.

Yamashita, Y.M., and Tumbar, T. (2014). Stem cells and their niche in homeostasis/regeneration and disease. Mol. Biol. Cell *25*, 736–736.

ACKNOWLEDGEMENTS

We thank C. Kimmel and V. Devasthali for feedback on the manuscript; the Stankunas lab for discussions; K. Poss and ZIRC for providing zebrafish lines; and the DSHB for antibodies.

Funding

The National Institutes of Health (NIH) provided research funding (1R01GM127761 (K. S. and S. S.) and 5R03AR067522 (S. S.)). G. A. Y. was supported by a NIH NRSA graduate fellowship (5F31AR071283). H.K.L. received support from the University of Oregon NIH-funded Developmental Biology Training Program (5T32HD007348).

Author contributions

S. S., G. A. Y., H. K. L. and K. S. designed experiments. S.S., G. A. Y., A. L. H., H. K. L., J. A. B., and J. C. performed experiments. K. S. and M. J. H. conducted the mathematical modeling. K. S. and S. S. prepared and wrote the manuscript with input from M. J. H., G. A. Y., H. K. L., and A. L. H.

Competing interests

None.

Data and material availability

RNA-Seq data are deposited at the NCBI Gene Expression Omnibus (GSE125859). Requests for materials should be addressed to S. S. and K. S.

Supplementary Materials

Materials and Methods
Figures S1-S9
Supplemental References

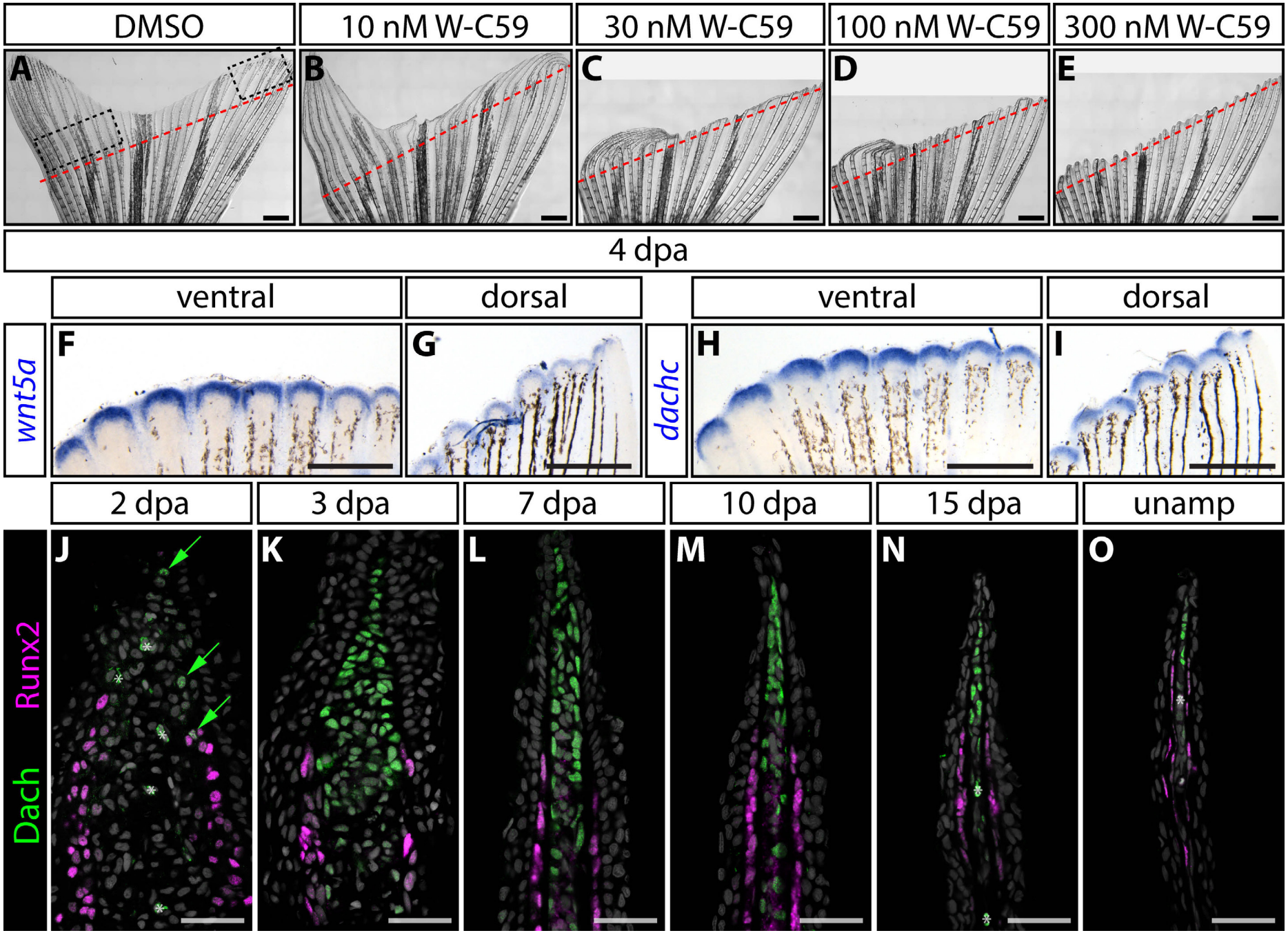

Figure 1. Dachshund transcription factors define Wnt-producing and growth-determining niche cells of regenerating fins.

Figure 1. Dachshund transcription factors define Wnt-producing and growth-determining
330 **niche cells of regenerating fins.**

(**A-E**) Sensitivity to Wnt inhibition inversely correlates with demand for regenerative growth. Diagonally fin-amputated zebrafish exposed to increasing concentrations of Wnt-C59 Porcupine inhibitor and imaged at 14 days post amputation (dpa). Red dashed lines show the amputation plane. Scale bars are 1 mm. (**F-I**) The size of distal *wnt5a* and *dachc* expression domains
335 positively correlate with regenerative demand following diagonal amputations. Images compare whole mount RNA in situ hybridization signal intensities between ventral (more proximal) and dorsal (more distal) sites along the diagonal resection plane, approximated by dashed boxes in (A). Scale bars are 500 μm. (**J-O**) Dachshund-expressing cells localize to the niche cells (a distal blastema population) distinct from adjacent Runx2-expressing progenitor osteoblasts.
340 Dach^{+} cells are first observed at 2 dpa, peak in number around 3 dpa, and then progressively decrease to a small residual pool that is also present in unamputated fins. Images show antibody-stained regenerating fin sections at the indicated times post-amputation. Dach (green) and Runx2 (magenta) expression. Hoechst-stained nuclei are grey. Asterisks denote red blood cells. Scale bars are 25 μm.

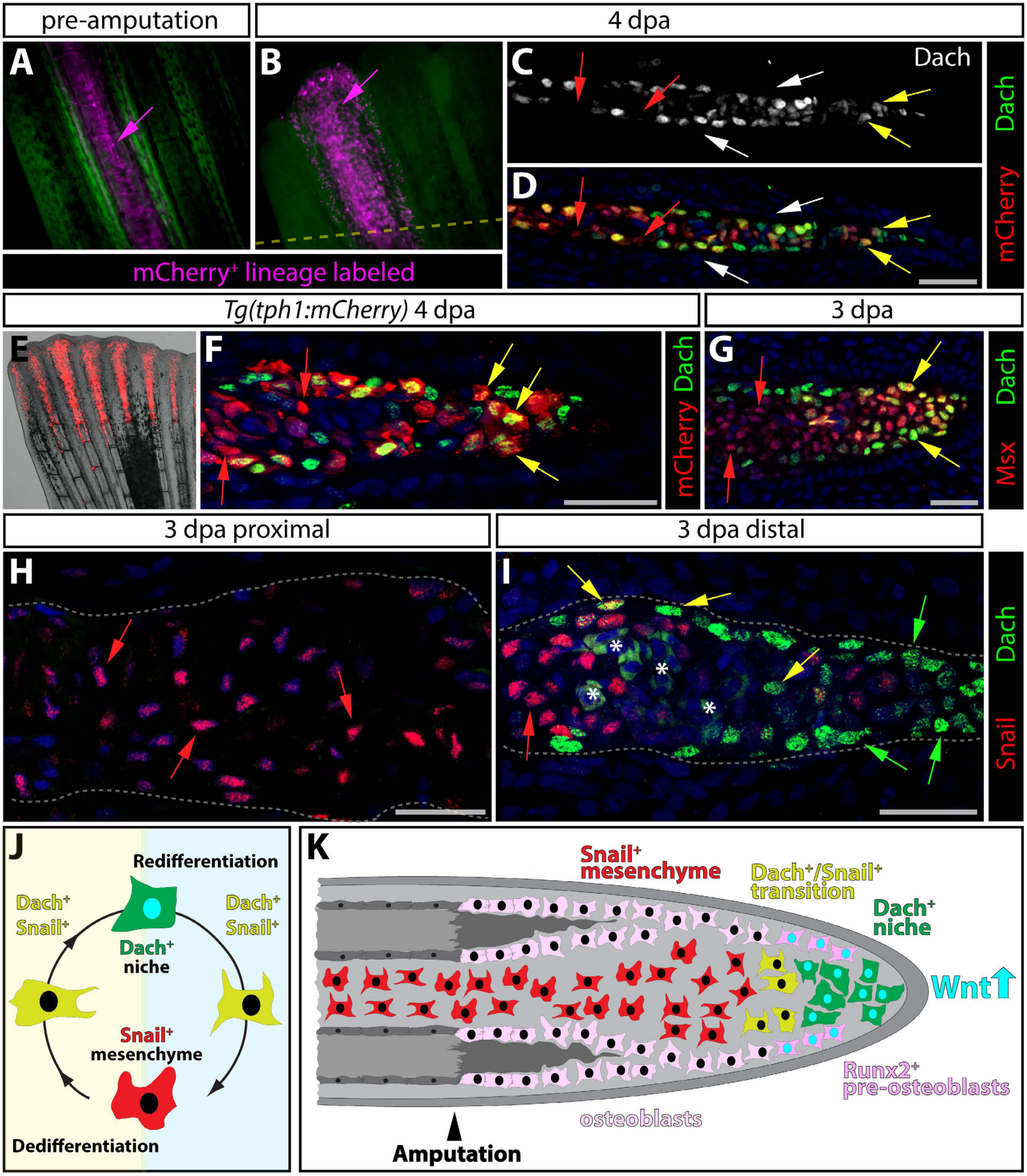

Figure 2. Niche cells are generated from state-transitioning intra-ray mesenchyme.

Figure 2. Niche cells are generated from state-transitioning intra-ray mesenchyme.

(A-D) Genetic mosaic analysis demonstrates that the Wnt-producing niche derives from intra-ray mesenchyme. Example of a genetic mosaic fin with a single ray containing mCherry-labeled mesenchyme (in magenta) prior to amputation (A) and 4 dpa (B). The amputation plane is
350 indicated with a dashed yellow line. (C, D) A section of the same ray at 4 dpa stained with anti-Dach (grey in single channel image in C, green in D) and anti-mCherry antibodies (red). Red arrows mark mCherry^{+} but Dach^{-} blastema cells, the yellow arrows highlight Dach^{+}/mCherry^{+} niche cells, and white arrows indicate unlabeled osteoblasts. **(E, F)** *Tg(tph1:mCherry)* expression highlights the regenerating intra-ray mesenchyme/niche lineage. Immunostaining of a 4 dpa
355 *Tg(tph1:mCherry)* fin section demonstrates Dach (green) expressing niche cells (yellow arrows) also express *tph1* (red). Red arrows mark proximal Dach^{-} *tph1*$^{+}$ mesenchyme. **(G-I)** Mesenchymal-to-niche cell transitions at 4 dpa defined by Dach, Msx, and Snail transcription factors. (G) Like *tph1:mCherry*, Msx expression (red) labels the lineage whether in a differentiated mesenchyme (red arrows) or Dach-expressing (green) progenitor niche (yellow
360 arrows) state. (H, I) Snail expression (red nuclei shown with red arrows) marks intra-ray mesenchyme proximal to the amputation site and blastema cells except distal Dach^{+} niche cells (green nuclei highlighted by green arrows). A small number of Snail^{+}/Dach^{+} cells (yellow nuclei indicated by yellow arrows) identify cells transitioning between mesenchyme and niche states. Scale bars in all panels are 25 μm. Asterisks denote red blood cells. **(J)**. Model of cell state
365 transitions between intra-ray mesenchyme and niche cells during regeneration. Snail^{+} mesenchyme cells normally populate the intra-ray space. After amputation, Snail^{+} cells dedifferentiate into Dach^{+} niche cells. As bone outgrowth proceeds, niche cells redifferentiate to restore Snail+ intra-ray mesenchyme. **(K)** Control of regeneration by a Wnt-producing dynamic

niche pool. Runx2^{+} osteoblasts (in pink) are maintained by Wnt (represented by cyan nuclei)
370 secreted by the distal Dach^{+}/Wnt^{+} niche (green cells with cyan nuclei), which transition (yellow cells) back to Snail^{+} mesenchyme (red cells) as regeneration progresses.

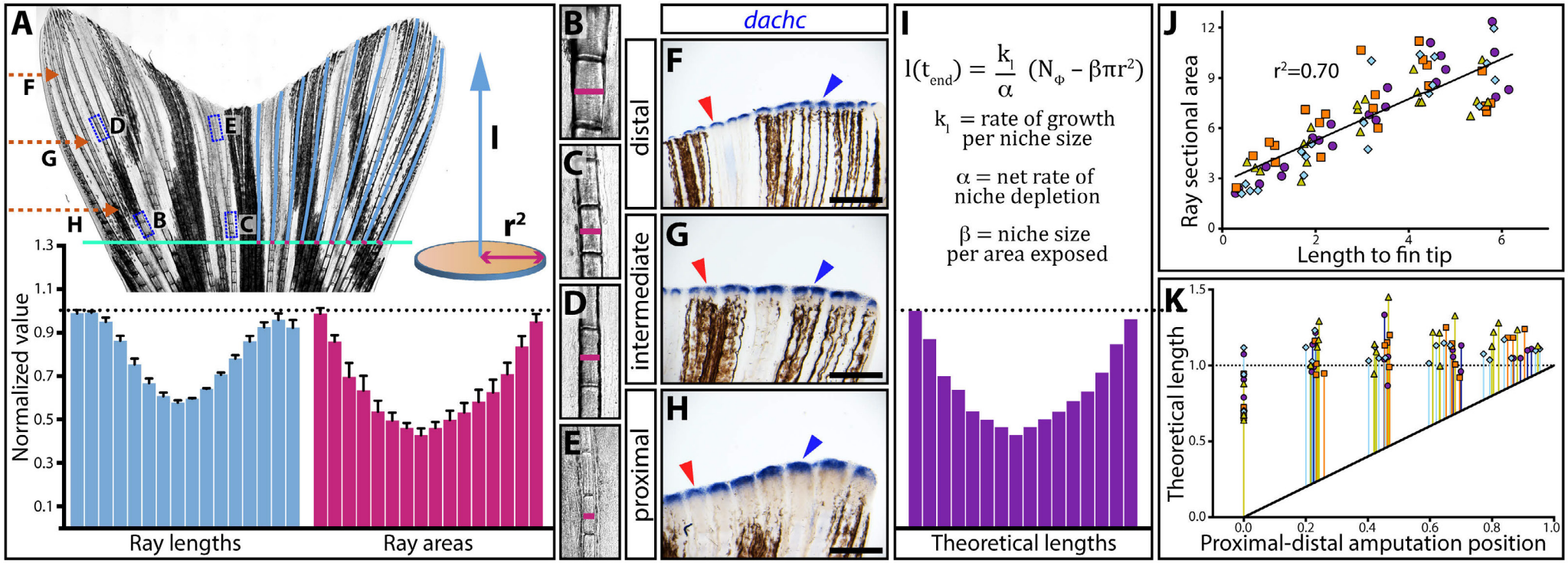

Figure 3. Skeletal geometry-dependent niche generation with progressive niche depletion directs regenerated ray length.

Figure 3. Skeletal geometry-dependent niche generation with progressive niche depletion directs regenerated ray length.

375 **(A)** A ray's surface area (or volume) exposed upon amputation (modeled by the square of the radius, r^2, pink) anticipates the length (l, light blue) it will regenerate. Plotted normalized measurements for the sixteen medial rays show a tight correlation between ray lengths and ray areas, from/at a hypothetical proximal amputation position (green line). Error bars are one standard deviation (n=4). (**B-E**) Scale-matched zoom images of the ray segments boxed in the 380 stitched whole fin image in (A), showing differential girth depending on bone position. Pink lines mark ray diameters. **(F-H)** *dachc* whole mount in situ hybridizations on 72 hpa regenerating fins amputated at distal (F), intermediate (G), or proximal (H) positions. As anticipated by the model, *dachc* expression, representing the amount of niche generated, correlates with regenerative demand. Scale bars are 500 μm. **(I)** A mathematical model equation 385 represents the length of a given ray at the end of regeneration ($l(t_{end})$) as a function of the radius of the ray at the amputation position. Three regulatory parameters (k_l, α, and β) must be tuned precisely to restore the original length, but no molecular positional information is required. The plot shows how the formula theoretically restores normalized ray lengths using actual measured radius values at the hypothetical amputation point (beige line). **(J)** Scatter plot showing a linear 390 relationship between ray sectional area and ray length from any measured position along the entire proximal-distal (P-D) fin axis. Each point represents 5 or 6 measured points from each of rays 3, 4, 15, 16 from four animals. Matching data point colors/shapes indicates a given ray. **(K)** The mathematical model predicts regenerated length (normalized = 1) regardless of amputation position. Each data point shows the theoretical length derived from a given ray's radius

395 measurements at one P-D position. The colored vertical lines represent anticipated growth from the amputation position (therefore, starting from the black diagonal line).

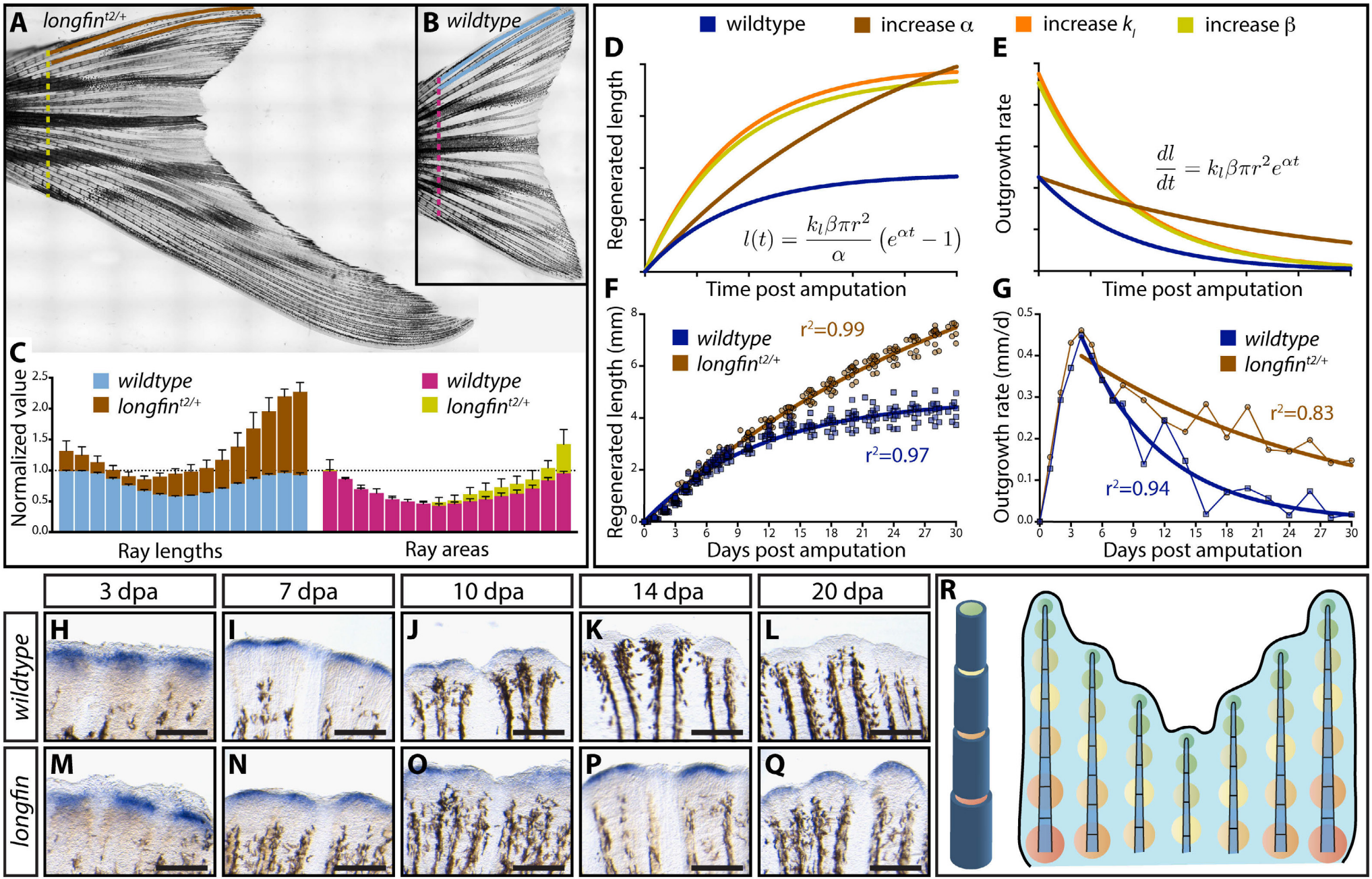

Figure 4. longfin fish regenerate exceptionally long fins due to a broken niche countdown timer, supporting a transpositional scaling model of self-restoring fin geometry.

Figure 4. *longfin* fish regenerate exceptionally long fins due to a broken niche countdown timer, supporting a transpositional scaling model of self-restoring fin geometry.

(A, B) Stitched differential interference contrast images show the dramatically overgrown caudal fins of *longfin*$^{t2/+}$ fish. Ray length and radius measurements taken at/from a proximal position denoted by colored dashed lines (brown/yellow=*longfin*$^{t2/+}$, light blue/pink=wildtype). **(C)** Normalized caudal fin ray lengths (left) and transverse areas (from *radius*^{2} measurements, right) for clutchmate wildtype and *longfin*$^{t2/+}$ fish. *longfin* fish have nearly the same ray areas as wildtype fish in spite of their much longer fin rays. This suggests one of the regulatory parameters is altered in *longfin* mutants. **(D)** Theoretical regeneration growth and **(E)** growth rate curves derived from the transpositional scaling equation have distinct shapes depending if niche response (k_l) or niche generation (β) vs. niche perdurance (α) parameters are increased. The actual growth **(F)** and growth rate **(G)** of regenerating *longfin*$^{t2/+}$ caudal fins match expectations if niche perdurance (α) – the "countdown timer" – is disrupted. The initial and maximum growth rate is unaltered but the growth rate progressively decreases at a much slower rate. Curves show actual data fit to the modeling equations (r square goodness of fit values are shown). All data points (≥ 12 fish per time) are shown in (F); points in (G) are mean values. (**H-Q**) Whole mount in situ hybridization for the *dachc* niche marker through a time course post-caudal fin amputation for wildtype and *longfin*$^{t2/+}$ fish. As the modeling predicts, *longfin*$^{t2/+}$ fish generate a normal-sized niche after fin resection but the cells fail to deplete in a timely manner. Scale bars are 200 μm. **(R)** A "transpositional scaling" model explains how positional information stored in skeletal geometry alone combined with a state transitioning and depleting niche population directs the fin to regenerate back to the original size and shape. A wider amputated ray produces more niche cells from its intra-ray mesenchyme. Niche cells deplete at a constant rate through their re-

differentiation to mesenchyme. The diminishing niche maintains a progressively smaller bone progenitor pool, regenerating a tapered ray and inherently restoring the geometry primed for future injury responses.